A New Tube Detection Filter for Abdominal Aortic Aneurysms

Erik Smistad[1,2], Reidar Brekken[2], Frank Lindseth[1,2]

[1] Norwegian University of Science and Technology, Trondheim, Norway.
[2] SINTEF Medical Technology, Trondheim, Norway.

Abstract. Tube detection filters (TDFs) are useful for segmentation and centerline extraction of tubular structures such as blood vessels and airways in medical images. Most TDFs assume that the cross-sectional profile of the tubular structure is circular. This assumption is not always correct, for instance in the case of abdominal aortic aneurysms (AAAs). Another problem with several TDFs is that they give a false response at strong edges. In this paper, a new TDF is proposed and compared to other TDFs on synthetic and clinical datasets. The results show that the proposed TDF is able to detect large non-circular tubular structures such as AAAs and avoid false positives.

1 Introduction

Tube detection filters (TDFs) are used to detect tubular structures in 3D images. They perform a shape analysis on each voxel and return a value indicating the likelihood of the voxel belonging to a tubular structure. The likelihood can be used for segmentation and centerline extraction of tubular structures such as abdominal aortic aneurysms from medical images. The segmentation and centerline of these structures are useful for visualization, volume estimation, registration and planning and guidance of vascular interventions.

Many TDFs use second order derivative information to perform the shape analysis like the eigenanalysis of the Hessian matrix. The eigenvalues of this matrix can be used to determine the shape of the local structure and the eigenvectors can be used to find the shape's orientation. To calculate the Hessian matrix at a voxel inside a tubular structure, the gradient information from the edges has to be present. For small tubular structures this is not a problem, but for large ones the gradients have to be propagated from the edges to the center. One way to do this is to compute the Hessian matrix in a Gaussian scale space by convolution with a Gaussian of different standard deviations. The final TDF measure is calculated as the maximum response over all scales. One problem with using Gaussian scale space is that on larger scales objects diffuse into each other and small tubular structures that are close to one another can diffuse together and give the impression that a larger tubular structure is present. Bauer

This is a preprint. The final publication is available at Springer via `http://dx.doi.org/10.1007/978-3-319-13692-9_22`

and Bischof [2] suggested to replace the gradient vector field from the Gaussian scale space with an edge-preserving diffusion process called gradient vector flow (GVF), originally introduced by Xu and Prince [13] as an external force field to guide active contours. With the GVF, only one scale is needed and the problem of objects diffusing into each other is avoided.

Frangi et al. [6] introduced a TDF called a vesselness filter. This filter uses the eigenvalues (λ) of the Hessian matrix to determine whether the current voxel $\boldsymbol{x}$ is part of a tubular structure. With the three measures $R_a = |\lambda_2|/|\lambda_3|$, $R_b = |\lambda_1|/\sqrt{|\lambda_2\lambda_3|}$ and $S = \sqrt{\lambda_1^2 + \lambda_2^2 + \lambda_3^2}$ the vesselness filter is defined in (1).

$$T_v(\boldsymbol{x}) = \begin{cases} 0 & \text{if} \quad \lambda_2 > 0 \quad \text{or} \quad \lambda_3 > 0 \\ (1 - e^{-\frac{R_a^2}{2\alpha^2}}) e^{-\frac{R_b^2}{2\beta^2}} (1 - e^{-\frac{S^2}{2c^2}}) & \text{else} \end{cases} \tag{1}$$

Frangi et al. used Gaussian scale space methods to do the multi-scale filtering, however Bauer et al. [2–4] later used the vesselness TDF successfully with the GVF.

The circle fitting TDF introduced by Krissian et al. [8] uses the eigenvectors of the Hessian matrix to identify the tubes cross-sectional plane. In this plane a circle is fitted to the underlying edge information. The fitting procedure samples N points on a circle with radius r and calculates the average dot product (2) of the edge direction ($\boldsymbol{V}$) and the circle's inward normal ($-\boldsymbol{d}_i$). The radius is gradually increased and the radius with the highest average is selected. The TDF response is then equal to the average with the select radius r as in (2).

$$T_{cf}(\boldsymbol{x}) = \frac{1}{N} \sum_{i=0}^{N-1} \boldsymbol{V}(\boldsymbol{x} + r\boldsymbol{d}_i) \cdot (-\boldsymbol{d}_i) \tag{2}$$

As a measure of edge direction, Krissian et al. [8] used the gradient calculated at the scale corresponding to the current radius. Bauer et al. [5] used the GVF field instead. Since this TDF assumes that the cross-sectional profile of the tubular structure is circular, it produces a lower response for non-circular tubular structures. Also, the cross-section of a tube is estimated using the eigenvectors of the Hessian matrix which are not accurate, hence even if the tubes are circular the cross-section may often appear as ellipses instead. Furthermore, the circle fitting TDF can give response in voxels where there is not a tubular structure. A semi-circle with a very high contrast can be enough to give a medium response. Pock et al. [9] proposed a symmetry measure to reduce the false response at such edges. This measure reduces the TDF response where the gradient's magnitude, i.e. the contrast, differs along the circle. However, this also reduces the response for tubular structures with a non-circular cross-section. Bauer [1] concluded in his thesis that several TDFs, including the vesselness and circle fitting TDF, have the problem that the response decreases significantly when the cross-section of the tubular structure deviates from a circle, which makes these tubular structures hard to distinguish from noise in the TDF response.

In this paper, a new TDF is proposed that uses GVF and is able to properly detect non-circular irregular tubular structures and reduce the amount of false

responses. In addition, it is demonstrated that a multigrid method is necessary for calculating the GVF for large tubular structures such as abdominal aortic aneurysms (AAAs).

2 Methods

Previously, we have developed a framework for extracting airways and blood vessels from different image modalities (e.g. CT, MR and US) using tube detection filters [10]. The framework consists of five main steps that are all executed on the graphic processing unit (GPU) (see Fig. 1) . The first step is to crop the volume in order to reduce the total memory usage. The second step involves some pre-processing, such as Gaussian smoothing and gradient vector flow, which are necessary to make the results less sensitive to noise and differences in tube contrast and size. After pre-processing, the TDF is performed. From the TDF result, the centerlines are extracted and finally, a segmentation is performed with a region growing procedure using the centerlines as seeds. The entire implementation is available online. Previously, the circle fitting TDF by Krissian et al. [8] was used in this framework. In this paper, a new TDF is proposed as a replacement for this filter to improve detection of large non-circular tubular structures and avoid detection of false tubular structures.

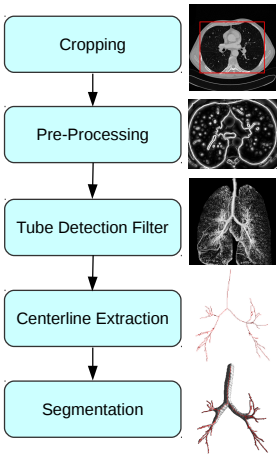

Fig. 1. Block diagram of the implementation

2.1 Large Tubular Structures and Gradient Vector Flow

The most common way to calculate GVF is to use Euler's method as demonstrated by Xu and Prince [13]. However, this method is very slow to converge [7]. And for large tubular structures where the gradients at the edges have to diffuse a long way to the center, this becomes a problem (see Fig. 3). To solve this problem, Han et al. [7] used multigrid methods to calculate GVF and achieved a much better convergence rate. In this paper, a GPU implementation of this multigrid method was used [11].

2.2 A New TDF for Non-Circular Tubular Structures

Like the circle fitting TDF, the proposed TDF uses the eigenvectors of the Hessian matrix to identify the orientation of the tubular structures. The two eigenvectors associated with the eigenvalues of the largest magnitude $\boldsymbol{e}_2$ and $\boldsymbol{e}_3$ span

http://github.com/smistad/Tube-Segmentation-Framework/

the cross-sectional plane of the tubular structure. In this plane, N line searches are performed from the current voxel $\boldsymbol{x}$ at different angles. For each line search i, a phasor is used to create vectors $\boldsymbol{d}_i$ that define the search direction θ.

$$\theta_i = \frac{2\pi i}{N} \qquad \boldsymbol{d}_i = \boldsymbol{e}_2 \sin\theta_i + \boldsymbol{e}_3 \cos\theta_i \tag{3}$$

Each line search continues until the edge of the tubular structure is encountered and the distance from the center to the edge for line search i is r_i. The edges are detected as the first peak in the vector field's magnitude above the fixed threshold 0.01. This threshold states the minimum gradient magnitude of an edge of a tubular structure. Thus, the value of 0.01 will allow most edges, but it is necessary to eliminate noise. If a dataset has noise with a higher contrast, this threshold may be increased. The problem of detecting false tubular structures is reduced by limiting the length of the line searches with a parameter $r_{\max}$. However, when detecting very large tubular structures, such as AAAs, $r_{\max}$ has to be set high and thus might not reduce the number of false positives. Also, if only large tubular structures are to be detected, a parameter, $r_{\min}$, can be set which sets the lower bound for the radius of the tubular structures to be detected. Using these distances, a measure $C(\boldsymbol{x})$ is created of how likely it is that the voxel $\boldsymbol{x}$ is in the center of the tubular structure (4). This measure enables the proposed TDF to be used for extracting centerlines and was also used by Wink et al. [12].

$$C(\boldsymbol{r}) = \frac{2}{N} \sum_{i=0}^{N/2-1} \frac{\min(r_i, r_{N/2+i})}{\max(r_i, r_{N/2+i})} \tag{4}$$

Finally, the TDF measure T is defined as the product of the center likelihood measure C and a measure M of how well the gradient vectors at the border correspond to the direction of the tubular structure $\boldsymbol{e}_1$.

$$M(\boldsymbol{x}) = \frac{1}{N} \sum_{i=0}^{N-1} (1 - |\boldsymbol{V}^n(\boldsymbol{x} + r_i \boldsymbol{d}_i) \cdot \boldsymbol{e}_1|) \tag{5}$$

$$T(\boldsymbol{x}) = \begin{cases} 0 & \text{if} \quad \exists i \boldsymbol{V}^n(\boldsymbol{x} + r_i \boldsymbol{d}_i) \cdot (-\boldsymbol{d}_i) < 0 \\ C(\boldsymbol{r}) M(\boldsymbol{x}) & \text{else} \end{cases} \tag{6}$$

Ideally, the gradient vectors $\boldsymbol{V}$ should be perpendicular to the direction of the tubular structure. This can be checked by taking the dot product of the normalized vectors $\boldsymbol{V}^n$ and $\boldsymbol{e}_1$. The closer the dot product is to zero, the closer the two vectors are to being perpendicular. At the borders of large tubular structures, the data will, locally, resemble more a plate structure than a tubular structure which may lead to an incorrect tube direction $\boldsymbol{e}_1$. The measure M thus reduces the response in the borders of the tubular structure where the tube direction $\boldsymbol{e}_1$ may be incorrect. This greatly improves the centerline extraction which uses the tube direction $\boldsymbol{e}_1$ [10]. Also, if there exist a vector that is more than 90° from the direction to the center $-\boldsymbol{d}_i$, the TDF measure is set to 0. This is done to further reduce the amount of false responses in which the edge gradient has another

direction than towards the center and is similar to the circularity measure used by Pock et al. [9].

3 Results

In this section, results of the proposed TDF are presented for both synthetic and clinical data and compared to the vesselness and circle fitting TDF in conjunction with GVF. The parameters used for the GVF are $\mu = 0.1$ with 6 iterations. The vesselness TDF was run with the parameters $\alpha = 0.5$, $\beta = 0.5$ and $c = 100$. And the circle fitting TDF used 32 sample points and the proposed TDF used $N = 12$ line searches.

Synthetic Data: A dataset containing tubular structures with different types of cross-sectional profiles was created. The profiles are displayed in the top of Fig. 2. This dataset contains tubular structures with circular, elliptical, several irregular profiles and one false tubular structure. The vesselness, circle fitting and proposed TDF were performed on this dataset. The responses along a line going through the middle of all of these tubular structures were recorded and are displayed as graphs in Fig. 2. The figure shows that the response of the circle fitting TDF is considerably reduced when performed on tubular structures with a non-circular cross-section, while the proposed TDF detects these almost as well as the circular structure. The circle fitting TDF also has a high response at the false tubular structure to the far right.

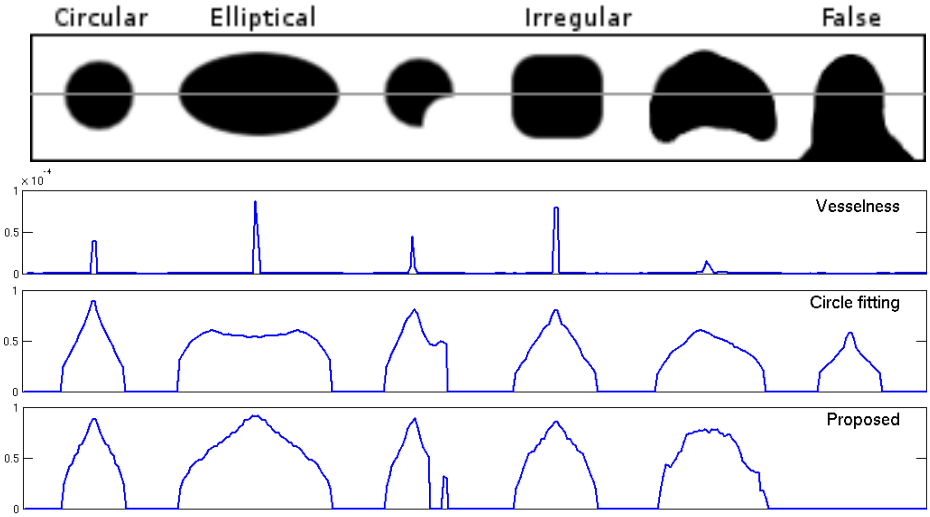

Fig. 2. The top row shows the cross-section of five different tubular structures and one false tubular structure. The three graphs below are the responses from the vesselness, circle fitting and proposed TDFs respectively, measured in a line that goes through the middle of all the cross-sections (the grey line in the top row).

Clinical Data: The TDFs were also executed on clinical CT datasets of abdominal aortic aneurysms (AAAs). Figure 3 illustrates the need for the multigrid method when calculating the GVF on large tubular structures such as an AAA. The figure shows the magnitude of the vector field after running GVF using Euler's method with 1000 iterations (about 6 seconds) and the multigrid method with 6 iterations (about 1 second). From this figure, it is evident that GVF with Euler's method has problems with diffusing the gradients on the edge of the aneurysm to the center, which is necessary for the TDFs. Over 10 times more iterations would be needed to reach the center with Euler's method which would reduce performance considerably. However, with the multigrid method the gradients are diffused to the center in about 1 second.

Figure 4 shows a maximum intensity projection of the response for each TDF on a CT image of an AAA. The TDFs were all executed on the same GVF vector field thus requiring only one scale. The same window and level were used on the circle fitting and the proposed TDF as both of these TDF have responses from 0 to 1. Also, the minimum radius ($r_{\min}$) and maximum radius ($r_{\max}$) used were 7 and 45 mm. This enables visual comparison of the two TDFs and it is clear that the circle fitting TDF creates a weaker response in the aneurysm than the proposed TDF. Furthermore, the amount of noise, especially from the spine, is higher with the circle fitting TDF. A different level and window were used for the vesselness TDF as its range is exponential. However, the AAA was not detected with this filter.

Figures 5 and 6 depicts the results using three different algorithms on four different AAA CT images. For comparison, the first column in the figures shows the segmentation result using the seeded region growing segmentation method. However, as this method leads to segmentation leakage into the spine on all datasets, the centerline was not possible to extract. The middle and right column show the segmentation surface and centerlines obtained with the circle fitting and the proposed TDF using the framework from [10] and the multigrid GVF method [11]. Here, $r_{\min}$ and $r_{\max}$ were set to 2 and 45 mm respectively. The vesselness TDF was not able to detect the AAAs and was therefore not included. The datasets consisted of 388-420 slices with size 512x512. The runtime of the entire implementation (see Fig. 1) including the TDF, centerline extraction and segmentation for these datasets was 4-10 seconds using a modern AMD Radeon HD7970 GPU.

4 Discussion

The results shows that the proposed TDF is able to properly detect large non-circular tubular structures such as AAAs in CT images. Figures 5 and 6 show that seeded region growing fails to segment the AAAs due to leakage to the spine and the circle fitting TDF is not able to properly detect some of the AAAs that deviate most from a circular cross-sectional profile.

The response of the vesselness and circle fitting TDF is dependent on the contrast due to the use of eigenvalues (Eq. 1) and gradient (Eq. 2). However,

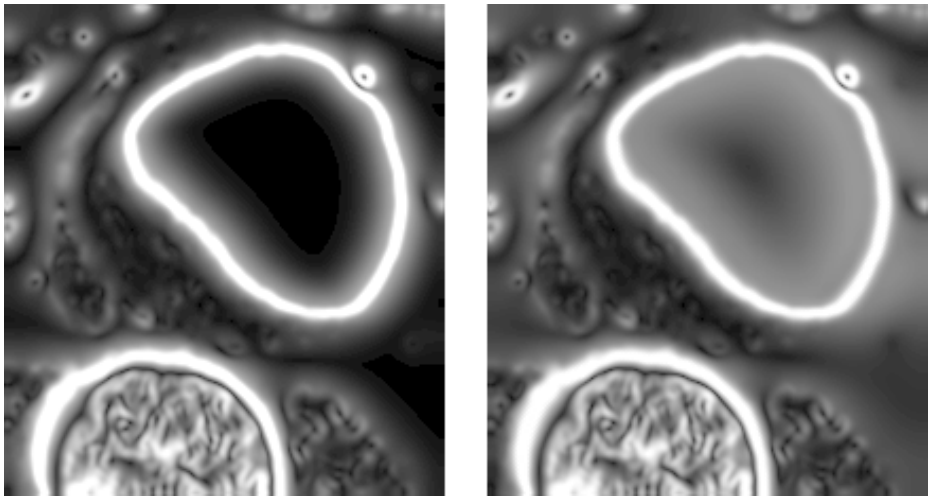

Fig. 3. Magnitude of the vector field after running gradient vector flow (GVF) on a AAA CT dataset. **Left:** Euler's method with 1000 iterations. **Right:** Multigrid method with 6 iterations. The image to the left shows that GVF with Euler's method has problems with diffusing the gradients on the edge of the aneurysm to the center which is necessary for the TDFs.

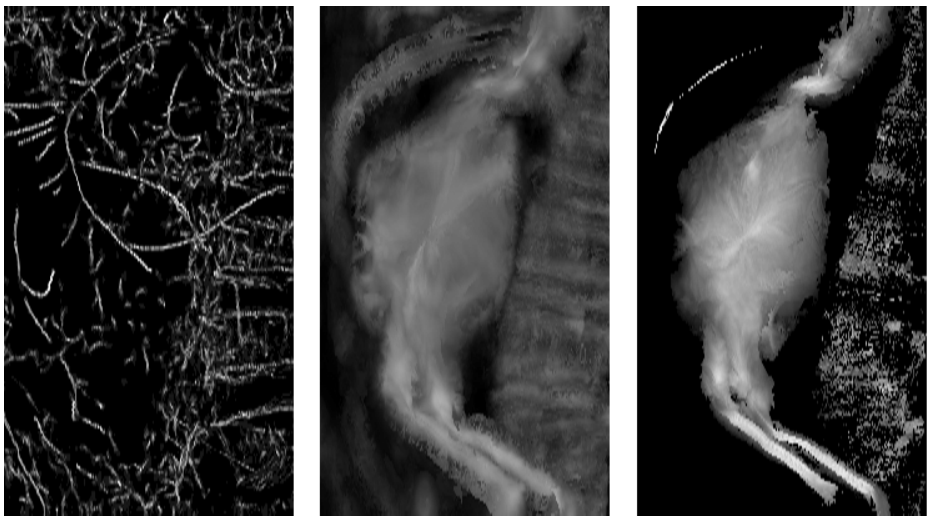

Fig. 4. Maximum intensity projection of TDF responses on a CT image of an abdominal aortic aneurysm (AAA) using the same GVF vector field. **Left:** Vesselness TDF. **Middle:** Circle fitting TDF. **Right:** Proposed TDF. The same level and window were used on the circle fitting and proposed TDF. A different level and window were used for the vesselness TDF as its range is exponential.

Fig. 5. Left: Region growing. **Middle:** Circle fitting TDF. **Right:** Proposed TDF.

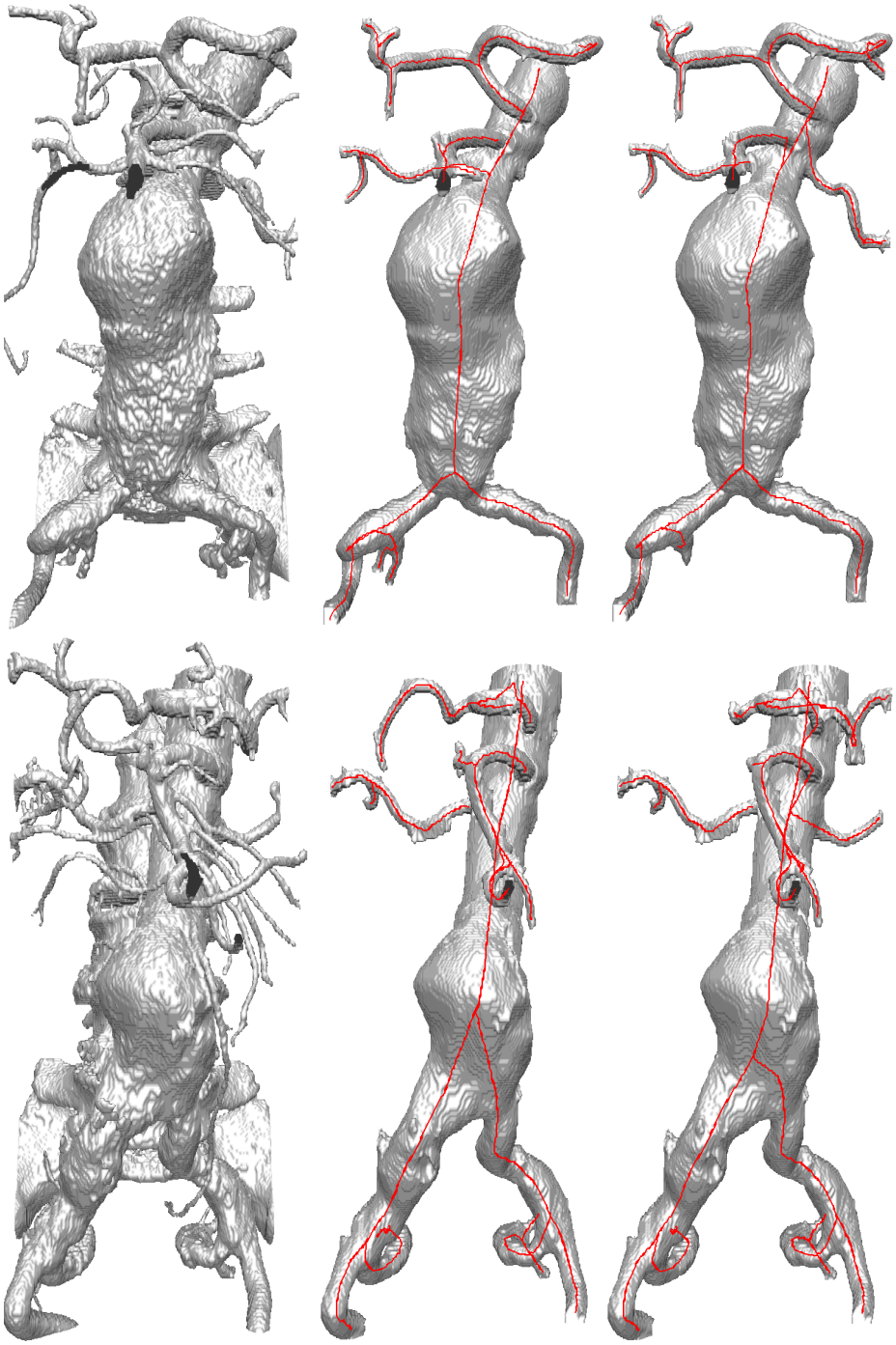

Fig. 6. Left: Region growing. **Middle:** Circle fitting TDF. **Right:** Proposed TDF.

the response of the proposed TDF is invariant to the contrast due to the use of the normalized gradient $\boldsymbol{V}^n$ in (5). Nevertheless, Bauer and Bischof [4] proposed a solution to this by adding a parameter $F_{\max}$ for the maximum contrast. Any gradient with a magnitude above this parameter would be normalized and any below, divided by this parameter. But this has also the effect of amplifying the effect of noise. The proposed TDF eliminates the need for this parameter.

5 Conclusions

A new tube detection filter using gradient vector flow was proposed and compared with two other commonly used filters. It was shown that the proposed filter is able to properly detect non-circular tubular structures such as abdominal aortic aneurysms and thus enable segmentation and centerline extraction of these structures.

References

1. Bauer, C.: Segmentation of 3D Tubular Tree Structures in Medical Images. Ph.D. thesis, Graz University of Technology (2010)
2. Bauer, C., Bischof, H.: A novel approach for detection of tubular objects and its application to medical image analysis. In: Proceedings of the 30th DAGM Symposium on Pattern Recognition. pp. 163–172. Springer (2008)
3. Bauer, C., Bischof, H.: Edge based tube detection for coronary artery centerline extraction. The Insight Journal (2008)
4. Bauer, C., Bischof, H.: Extracting curve skeletons from gray value images for virtual endoscopy. In: Proceedings of the 4th International Workshop on Medical Imaging and Augmented Reality. pp. 393–402. Springer (2008)
5. Bauer, C., Bischof, H., Beichel, R.: Segmentation of airways based on gradient vector flow. In: Proceedings of the 2nd International Workshop on Pulmonary Image Analysis. MICCAI. pp. 191–201. Citeseer (2009)
6. Frangi, A., Niessen, W., Vincken, K., Viergever, M.: Multiscale vessel enhancement filtering. Medical Image Computing and Computer-Assisted Interventation 1496, 130–137 (1998)
7. Han, X., Xu, C., Prince, J.: Fast numerical scheme for gradient vector flow computation using a multigrid method. Image Processing, IET (1), 48–55 (2007)
8. Krissian, K., Malandain, G., Ayache, N.: Model-Based Detection of Tubular Structures in 3D Images. Computer Vision and Image Understanding 80(2), 130–171 (Nov 2000)
9. Pock, T., Beichel, R., Bischof, H.: A novel robust tube detection filter for 3D centerline extraction. Image Analysis pp. 481–490 (2005)
10. Smistad, E., Elster, A.C., Lindseth, F.: GPU accelerated segmentation and centerline extraction of tubular structures from medical images. International Journal of Computer Assisted Radiology and Surgery 9(4), 561–575 (2014)
11. Smistad, E., Lindseth, F.: Multigrid gradient vector flow computation on the GPU (2014), manuscript submitted for publication.
12. Wink, O., Niessen, W.J., Viergever, M.a.: Fast delineation and visualization of vessels in 3-D angiographic images. IEEE transactions on medical imaging 19(4), 337–46 (Apr 2000)

13. Xu, C., Prince, J.: Snakes, shapes, and gradient vector flow. IEEE Transactions on Image Processing 7(3), 359–369 (1998)